Proceedings of the Seventh International Conference on
Railway Technology: Research, Development and Maintenance
Edited by: J. Pombo
Civil-Comp Conferences, Volume 15, Paper 3.13
Civil-Comp Press, Edinburgh, United Kingdom, 2026
ISSN: 2753-3239, doi: 10.4203/ccc.15.3.13

Development of Monitoring Technology on Wheel Flange Lubrication Condition With PQ Monitoring Bogie in Operation

T. Ueda[1], J. Kurihara[1], T. Saito[1], T. Watanabe[1], T. Matsuda[1], M. Tanimoto[2] and E. Miyauchi[2]

[1]Tokyo Metro Co., Ltd., Japan
[2]Metro Sharyo Co., Ltd., Japan

Abstract

The authors are developing the technology for monitoring the lubrication condition between outside wheel flange and rail gauge corners. To validate the evaluation method of lubrication condition, the new wear index proposed by Ichiyanagi et al. is applied as a lubrication condition index, and the forces acting between the wheel and the rail are measured using the PQ monitoring bogie on a curve where the amount of lubricant applied was varied. The lubrication condition index derived from the measurement results with the PQ monitoring bogie was validated, and it was found that the lubrication condition index can express changes in the lubrication condition of outside rail. And we also captured the phenomenon of increasing derailment coefficient with increasing the amount of lubricant applied.

Keywords: flange wear, rail-gauge corner wear, PQ monitoring bogie, wheel/rail contact, friction coefficient, lubrication, condition monitoring.

1 Introduction

In this study, the authors are developing the technology for monitoring the lubrication conditions of the wheel flange and outside rail gauge corners using the PQ monitoring bogie showed in Figure 1 [1], [2]. In urban subway systems, there are many sharp curves. When the train passes through the sharp curve, the outside wheel flange of leading axle contacts with rail gage corner, causing wear and squeaking noise. To prevent these phenomena, lubricant is applied at the contact points between the wheel flange and rail gauge corner. However, excessive lubrication can result in wheel slip or skid. Therefore, it is essential to monitor the lubrication condition between wheel flange and rail gage corner. Current monitoring methods, however, heavily rely on manual track inspections, which are labor intensive. To deal with these issues, the authors are developing the technology monitoring the lubrication condition between outside wheel flange and rail gage corner. This paper presents the development that evaluation of lubrication condition using the PQ monitoring bogie capable of measuring the forces acting between wheel and rail in operation line.

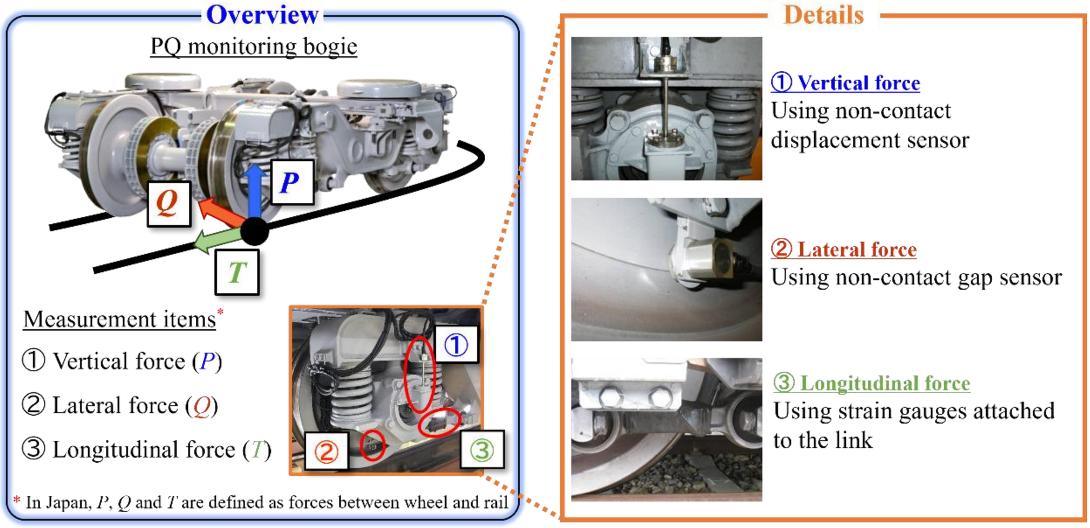

Figure 1: PQ monitoring bogie

2 Conventional studies of monitoring the lubrication condition between the wheel flanges and the rail gauge corner

Few studies on lubrication and friction between wheel flange and rail gage corner exist in the world. This is probably due to the lack of methods to measure them until recently. Iijima et al. observed the derailment coefficient at the limit where the wheel rides up on the rail and calculated the friction coefficient of the wheel flange from that value [3]. In contrast, Matsuda et al. attempted to determine the lubrication condition between wheel flange and rail gage corner using the PQ monitoring bogie [4]. When the wheel-rail interface is dry, the longitudinal force on the contact surface between wheel and rail increases. In contrast, when the wheel-rail interface is lubricated, the longitudinal force decreases. Focusing on this relationship, they have derived the ratio of the longitudinal force to the outside wheel load, namely, Tangential force coefficient using the PQ monitoring bogie. And they have evaluated the lubrication condition between outside wheel flange and rail gage corner using this coefficient as the lubrication condition index with full-scall roller-rig equipment. On the other hand, Ichiyanagi et al. proposed the index of the ratio of longitudinal force to lateral force acting on the inside rail to evaluate the outside wheel flange-rail wear. They have shown that this index can be an effective index for evaluating the outside wheel flange-rail wear through the results of roller-rig tests and Multi body Dynamics analysis.

3 The index for evaluating the wear of wheel flange [5]

3.1 Overview of the index

The index for evaluating the outside wheel flange-rail wear proposed by Ichiyanagi et al. is based on the idea of friction circle. This index is hereafter referred to as the new wear index. Figure 2 shows the relationship of forces between wheel and rail in the leading axle. And figure 3 shows the friction circles in different lubrication conditions between the leading-inside wheel and rail.

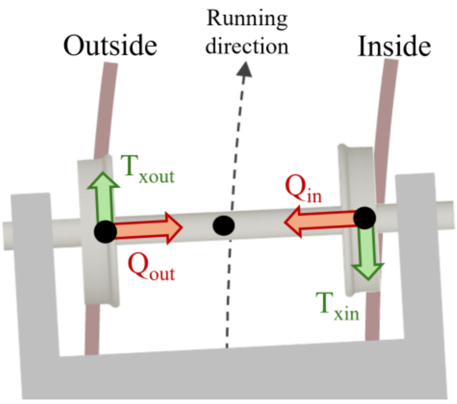

Figure 2: Relationship of forces between wheels and rails in the leading axle

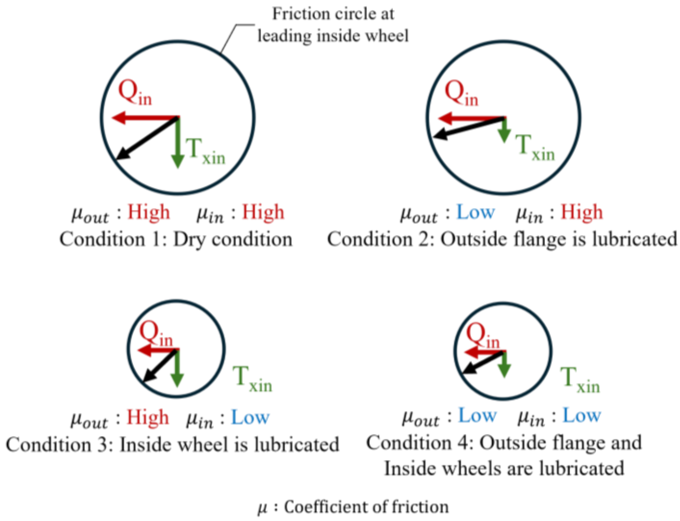

Figure 3: Friction circle at leading-inside wheel

In sharp curve, the tangential force saturates the radius of friction circle. And the radius of circle varies with the lubrication condition of inside rail. In figure 3, condition 1 and 2, lubrication conditions of inside wheel are dry. So, the radius of circles in condition 1 and 2 are larger than that of condition 3 and 4 because the friction coefficient is large in the leading-inside wheel. The effect of the outside wheel flange lubrication appears as a balance between the longitudinal force and lateral force in the leading-inside wheel. When the lubricant is applied to inside wheel, it is difficult to find a difference of longitudinal force between condition 3 and 4. But the direction of the balance between the longitudinal force and lateral force vector clearly changes. Focusing on this relationship, they proposed the ratio of the longitudinal force and lateral force in the leading-inside wheel as the wear index. This index is shown in Equation (1).

$$\frac{T_x}{Q_{in} \times R} \tag{1}$$

In Equation (1), Q_{in} means the lateral force in the leading-inside wheel, and R means the radius of curve. The ratio of the longitudinal force and inside lateral force is divided by curve radius to consider the difference in curve radius here. T_x means the average of the absolute values of the longitudinal force acting on the outside and inside rails in the curve and derived from Equation (2).

$$T_x = \frac{|T_{xout}| + |T_{xin}|}{2} \tag{2}$$

3.2 Validation for the wear index with roller-rig test and simulation

To validate the index shown in Equation (1), they have compared with the results of roller-rig test and simulation with multi-body dynamics analysis. Figure 4 shows the relation between the new wear index and relative wear in the roller-rig test. The relative wear is the percentage wear dust from wheel flange adhering to the Kent paper that is observed with an electric microscope. From this figure, when the new wear index is larger than about 2×10^{-3}, the relative wear increases as the new wear index increases.

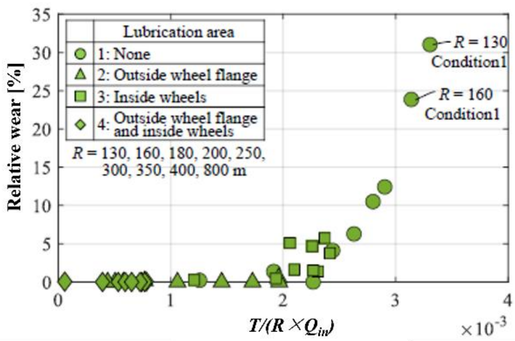

Figure 4: Relationship between the new wear index and relative wear in roller-rig test

Figure 5 shows simulation results showing the relationship between the new wear index and the wear number. The wear number $T\gamma$ is calculated as a sum of products from creep forces and creepages [6]. From this figure, correlation coefficient r is 0.97 that indicates a strong correlation between the new wear index and the wear number.

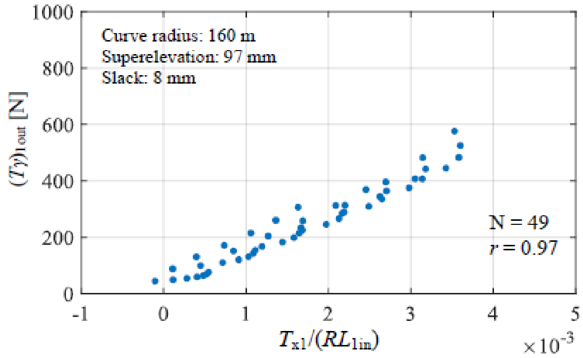

Figure 5: Relationship between the new wear index and wear number

From these results, they have said that the new wear index can be the effective index for evaluating the wear of the leading-outside wheel flange. In the present paper, the authors attempt to evaluate the lubrication condition between outside wheel flange and rail gage corner using the new wear index as the new lubrication condition index.

4 Validation of the new lubrication condition index in operation

4.1 Validation condition

To validate the effect of changing the lubrication condition between outside wheel flange and rail on the index, the authors have changed the lubrication condition on the rail of curve in operation and measured forces between the wheel and the rail using the PQ monitoring bogie. Figure 6 and Figure 7 show the details of the curve conditions in the validations.

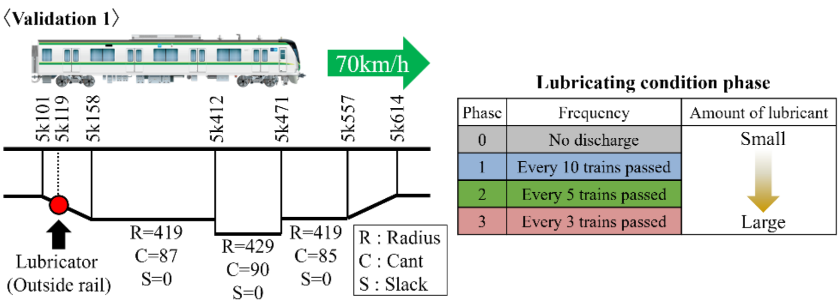

Figure 6: Validation conditions in operation line (Validation 1)

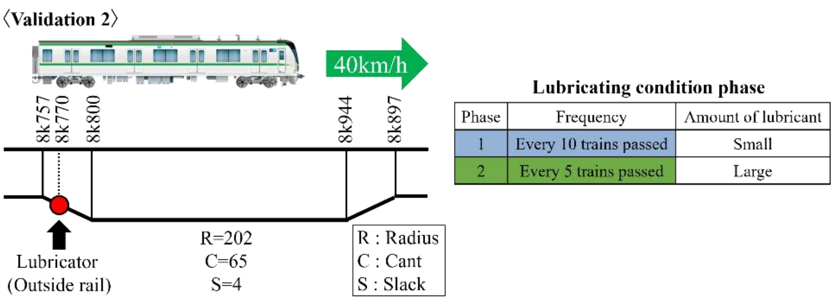

Figure 7: Validation conditions in operation line (Validation 2)

In validation 1, the curve has a radius range of 419 m to 429 m. In validation 2, the curve radius is 202 m. In both validations, the lubricators had been installed at the entrance of the outside curve. In validation 1, the authors had set 4 different lubrication condition phases. And in validation 2, the authors had set two different lubrication condition phases. In the PQ monitoring bogie, the gyro sensor measures the vehicle's angular rate of yawing ω. If the vehicle's running speed is υ, the curve radius R is given by the Equation (3).

$$R = \frac{\upsilon}{\omega} \tag{3}$$

4.2 Validation results

4.2.1 Transition of the new lubrication condition index in target curve

A comparison of the transition of the new lubrication condition index in validation 1 is shown in Figure 8, and validation 2 is shown in Figure 9. Horizontal axes of each graph show the kilo post in validation section. And the graph of first row from the top shows the new lubrication condition index, second row shows the average of longitudinal force, third row shows the ratio of the inside lateral force to the inside vertical force is known as the lubrication condition index of inside rail, and forth row shows the curvature. Changing the lubrication condition of the inside rail affects the longitudinal force. But we have judged there is no effect to longitudinal force because transition showed in third row are almost the same for each phase in validation 1 and 2. The comparison in these figures show that the new lubrication condition index value decreases as the amount of lubricant applied increases regardless of the curve radius.

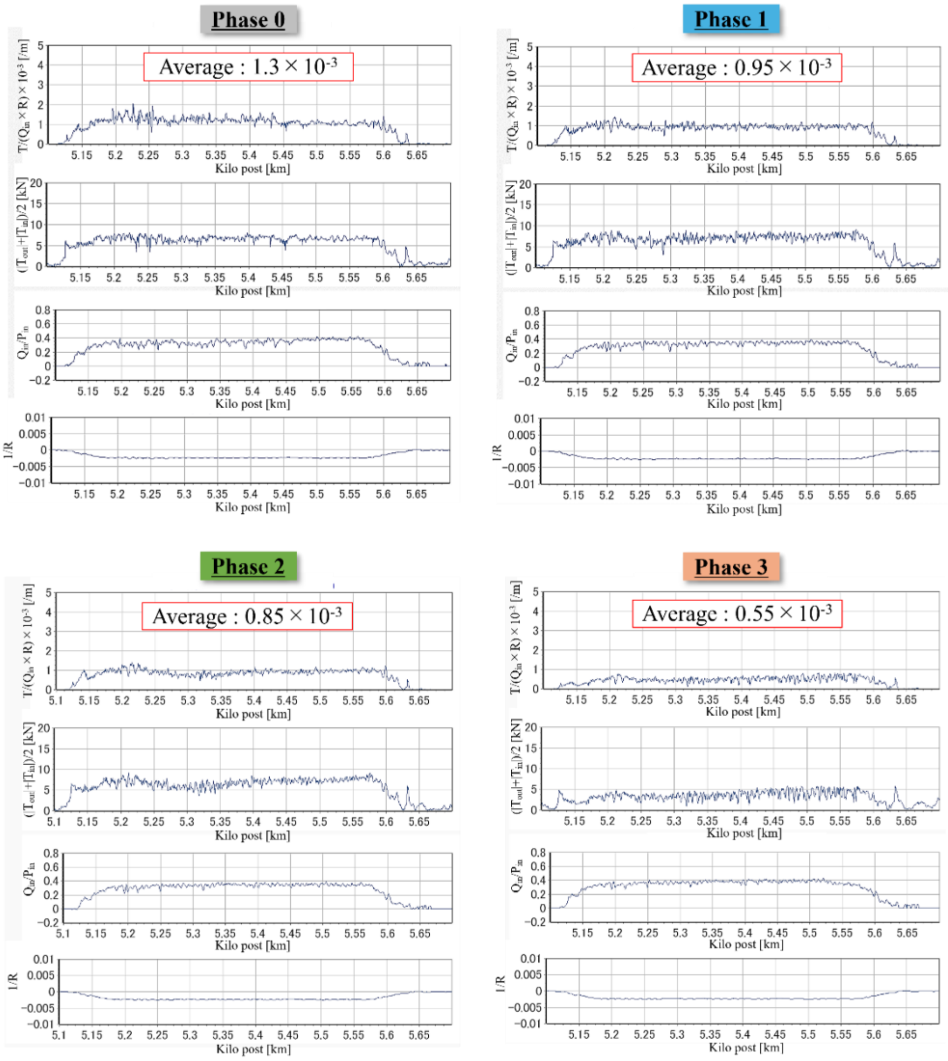

Figure 8: Comparison of the new lubrication condition index (Validation 1)

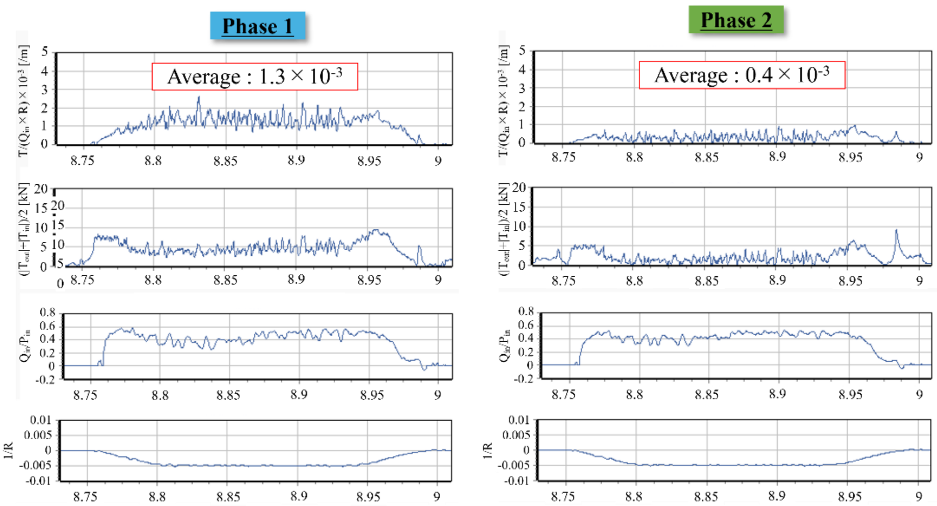

Figure 9: Comparison of the new lubrication condition index (Validation 2)

4.2.2 One-month transition of the new lubrication condition index

Figure 10 shows the one-month transition of the new lubrication condition index in validation 1. Each plot in Figure 10 is the value of the new lubrication condition index derived from the longitudinal force and the lateral force measured in the middle point of the target curve. From this figure, we can find that the new lubrication condition index tends to decrease gradually as the amount of lubricant applied increases.

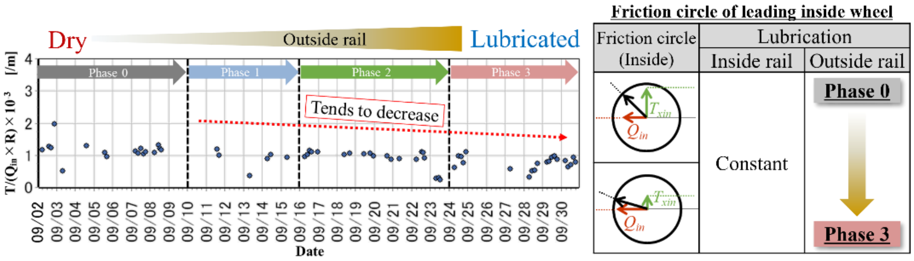

Figure 10: Transition of the new lubrication condition index in target curve (Validation 1)

Based on these results so far, we have validated that the new lubrication condition index can express changing in lubrication conditions of the outside rail in operation.

5 Increasing derailment coefficient

5.1 Estimation mechanism

Figure 11 shows the one-month transition of the derailment coefficient in the middle point of the target curve in Validation 1. And Figure 12 shows the one-month transition of the outside lateral force in the middle point of the target curve in Validation 1. From these, we can find that the derailment coefficient tends to increase because of increasing the outside lateral force as the amount of lubricant increases. We speculate that this phenomenon is due to decreasing longitudinal force.

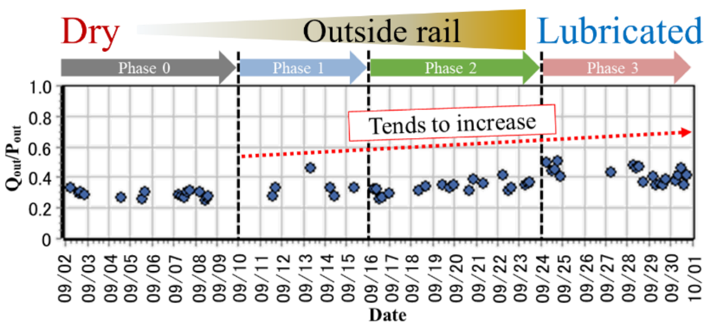

Figure 11: Transition of the derailment coefficient in the target curve (Validation 1)

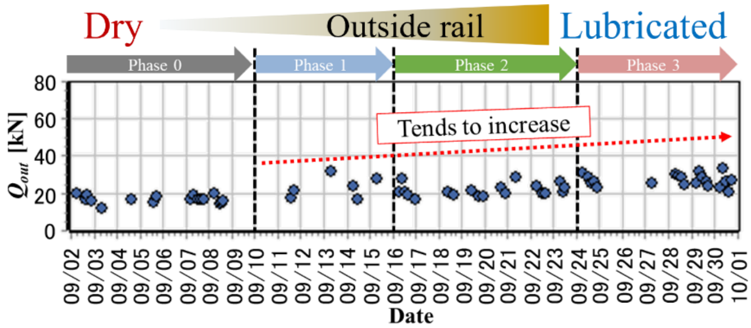

Figure 12: Transition of the outside lateral force in target curve (Validation 1)

Figure 13 shows the forces acting on the bogie during curve. When the outside rail is lubricated, the steering moment in leading axle is decreased due to decreasing the longitudinal force. On the other hand, Anti steering moment in trailing axle is almost the same as dry condition. Because there is no contact between wheel flange and rail in trailing axle. That is why the outside lateral force in leading axle tends to increase as the amount of lubricant increases.

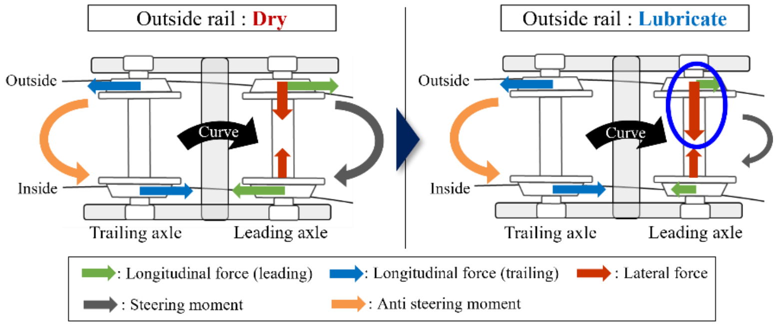

Figure 13: The forces acting on the bogie during curve

5.2 Critical derailment coefficient considering the friction coefficient

It is generally recognized that the risk of derailment increases as the derailment coefficient increases. Because when we assess the derailment coefficient, we compare to critical derailment coefficient with fixed friction coefficient. Equation 4 shows critical derailment coefficient based on Nadal formula. In this equation, θ means wheel flange angle. And μ_{out} means friction coefficient between the outside wheel flange and the rail.

$$\left(\frac{Q}{P}\right)_{cri} = \frac{tan\theta - \mu_{out}}{1 + \mu_{out} tan\theta} \tag{4}$$

On the other hand, Matsumoto et al. are proposed new safety index called "Flange Climb Index" [7]. This index is hereafter called the FCI. The FCI uses the critical derailment coefficient with estimated friction coefficient. Figure 14 shows the method of estimating friction coefficient proposed by Matsuda et al. [4]. To estimate friction coefficient, Estimator is constructed by Multibody Dynamics Analysis with specification of curve and vehicle. Using this estimator, μ_{out} can be estimated recursively from forces measured by the PQ monitoring bogie.

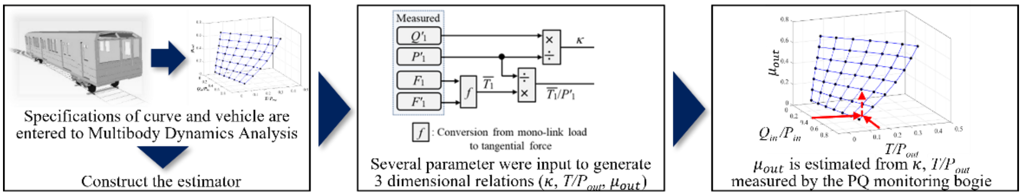

Figure 14: Estimation method of friction coefficient (Proposed by Matsuda et al.,)

Figure 15 shows the estimated friction coefficient in validation 1. And Figure 16 shows the critical derailment coefficient considering estimated friction coefficient in validation 1. We can find from these graphs that the critical derailment coefficient tends to increase because of decreasing the friction coefficient as the amount of oil increases.

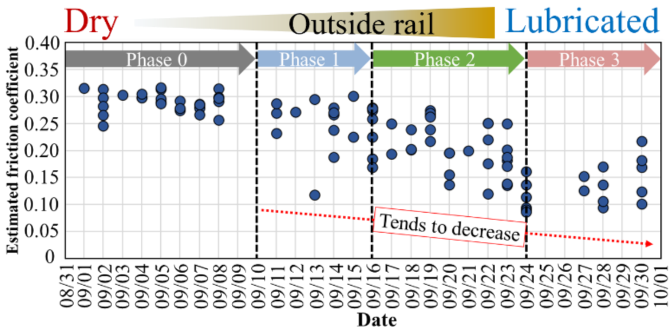

Figure 15: Estimated friction coefficient in validation 1

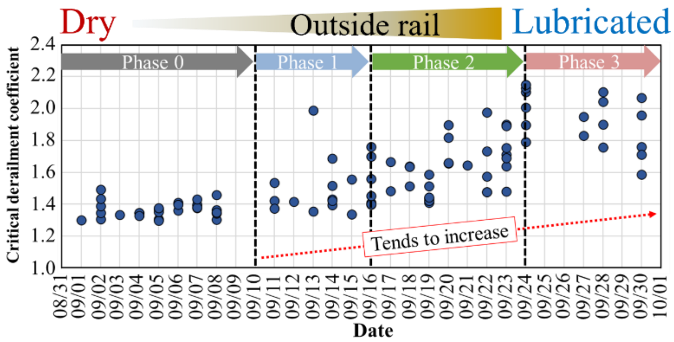

Figure 16: Critical derailment coefficient considering estimated friction coefficient in validation 1

Figure 17 shows the result of the FCI. From this figure, we can find that as the critical derailment coefficient increases with increasing lubricants, FCI's are consequently almost constant. So, we found out the possibility that the FCI is valid for derailment risk assessment on operation line.

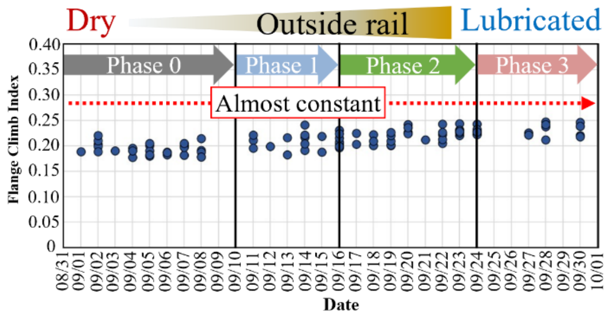

Figure 17: Transition of the FCI in target curve (Validation 1)

6 Conclusions and Contributions

As part of the development of technology to monitor the lubrication condition of the contact area between the wheel flange and the outside rail, the authors validated the evaluation method of the lubrication condition using the PQ monitoring bogie in operation. In our validation, the force acting between the wheel and rail was measured using the PQ monitoring bogie on the curves with changing amount of lubricant, and the new lubrication condition index were derived. As a result, it was confirmed that the new lubrication condition index can express changes in lubrication conditions of the outside rail on actual operation lines. Also in this validation, we captured the phenomenon of increasing derailment coefficient with increasing the amount of lubricant applied and found the possibility that the safety index of Matsumoto et al. are valid for operating lines as well.

Acknowledgements

This work was supported by Nihon University, National Traffic Safety and Environment Laboratory, Ibaraki University, Metro Sharyo Co., Ltd., and Nippon Steel Corporation.

References

[1] A Matsumoto., Y Sato., H Ohno., M Tomeoka., K Matsumoto., M Tanimoto., Y Sato: A new measuring method of wheel-rail contact forces and related considerations, Wear, 265(9-10), 1518-1525, 2008.

[2] H Taguchi., M Shimizu., T Saito., Y Sato., Y Oki., J Osakada., M Tanimoto: Assumption of Lateral/vertical/rail-interaction-force by simplified method (4th report; Advanced research in new measuring method of derailment coefficient), JSME Proceedings, No.09-65, 229-232, 2009.

[3] H Iijima., K Doi., K Muraki., R Imada., A Kataori., S Momosaki., S Matsumoto: Investigation into the cause of the low-speed ride-up derailment that occurred at the Oku Station and verification of countermeasures, JR EAST Technical Review (29), 21-26, 2009.

[4] T Matsuda., F Masuzawa., T Maeda., A Iwamoto., K Matsumoto., M Tanimoto., A Matsumoto., Y Michitsuji., Y Ichiyanagi., Y Sato., H

Ohno.， T Nakai: Estimation of friction coefficient between outside flange and rail surface， CM2018， 689-694， 2018.

[5] Y Ichiyanagi., Y Sato., Y Michitsuji., A Matsumoto., M Tanimoto., Y Nakasato., J Ito., T Matsuda., D Shinagawa: Evaluation of wheel flange lubrication condition based on continuous observation of wheel/rail contact forces， IAVSD 2023, Advances in Dynamics of Vehicles on Roads and Tracks III, 161-171, 2024.

[6] Polach, O. et al: Simulation of Railway Vehicle Dynamics, Handbook of railway vehicle dynamics second edition, ch.17, CRC Press, 707, 2020.

[7] A Matsumoto., Y Michitsuji., Y Ichiyanagi., Y Sato., H Ohno., M Tanimoto., A Iwamoto., T Nakai: Safety measures against flange-climb derailment in sharp curve-considering friction coefficient between wheel and rail, Wear, 432-433(3-4), 2019.